PHYTOTHERAPY RESEARCH
Phytother. Res. **22**, 169–179 (2008)
Published online 29 August 2007 in Wiley InterScience
(www.interscience.wiley.com) **DOI**: 10.1002/ptr.2277

Pharmacometrics of Pterostilbene: Preclinical Pharmacokinetics and Metabolism, Anticancer, Antiinflammatory, Antioxidant and Analgesic Activity

Connie M. Remsberg[1], Jaime A. Yáñez[1], Yusuke Ohgami[1], Karina R. Vega-Villa[1], Agnes M. Rimando[2] and Neal M. Davies[1]*

[1]Department of Pharmaceutical Sciences, and Pharmacology and Toxicology Graduate Program College of Pharmacy, Washington State University Pullman, Washington 99164-6534, USA
[2]Natural Products Utilization Research Unit, Agricultural Research Service, U.S. Department of Agriculture, PO Box 8048, University, Mississippi 38677, USA

The present study evaluated the preclinical pharmacokinetics and pharmacodynamics of *trans*-pterostilbene, a constituent of some plants. Right jugular vein cannulated male Sprague-Dawley rats were dosed i.v. with 20 mg/kg of pterostilbene and samples were analysed by the reverse phase HPLC method. Serum AUC, serum $t_{1/2}$, urine $t_{1/2}$, Cl_{total} and Vd_{β} were 17.5 ± 6.6 μg/h/mL, 1.73 ± 0.78 h, 17.3 ± 5.6 h, 0.960 ± 0.025 L/h/kg and 2.41 ± 1.13 L/kg (mean ± SEM), respectively. A pterostilbene glucuronidated metabolite was detected in both serum and urine. The *in vitro* metabolism in rat liver microsomes furthermore suggests phase II metabolism of pterostilbene. Pterostilbene demonstrated concentration-dependent anticancer activity in five cancer cell lines (1–100 μg/mL). An *in vitro* colitis model showed concentration-dependent suppression of PGE_2 production in the media of HT-29 cells. Antiinflammatory activity was examined by inducing inflammation in canine chondrocytes followed by treatment with pterostilbene (1–100 μg/mL). The results showed decreased levels of MMP-3, sGAG and TNF-α compared with control levels. Pterostilbene exhibited concentration-dependent antioxidant capacity measured by the ABTS method. Pterostilbene increased the latency period to response in both tail-flick and hot-plate analgesic tests. Copyright © 2007 John Wiley & Sons, Ltd.

Keywords: pharmacokinetics; pterostilbene; stilbene; anticancer; antiinflammatory; colitis.

INTRODUCTION

Pterostilbene (*trans*-3,5-dimethoxy-4′-hydroxystilbene), $C_{16}H_{16}O_3$, MW 256.296 g/mol, XLog P = 4.1 (Fig. 1A) is a naturally occurring stilbenoid compound derived from the phenylpropanoid pathway (Kodan *et al.*, 2002). It is a structural analogue of another highly studied stilbene, resveratrol (Fig. 1B), which has demonstrated anticancer activity, antioxidant capacity, antiinflammatory activity, and possesses other potential health benefits (Fremont, 2000).

Pterostilbene has been isolated from several natural plant sources including several types of grapes (Adrian *et al.*, 2000; Douillet-Breuil *et al.*, 1999; Pezet and Pont, 1988) and deerberry and rabbiteye blueberries (Rimando *et al.*, 2004). Other reports of pterostilbene identification include several plants used in traditional medicine. Two such plants are used in Ayurvedic medicine: *Pterocarpus marsupium*, a tree whose heartwood is used as a treatment for diabetes (Manickam *et al.*, 1997) and darakchasava, a medicinal drink

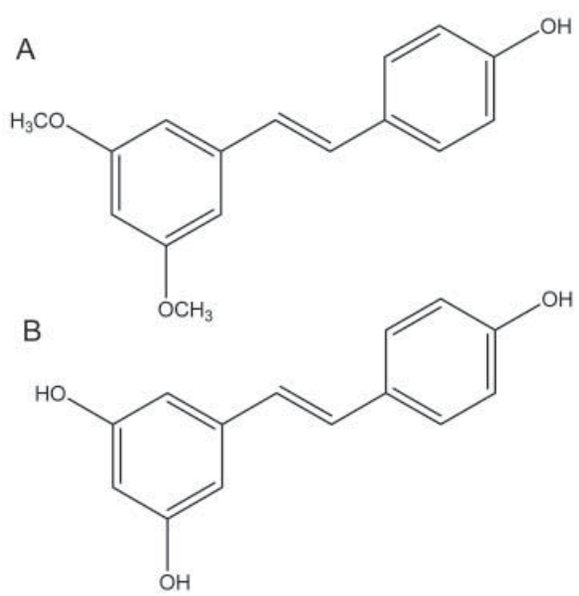

Figure 1. (A) Chemical structure of pterostilbene; (B) chemical structure of resveratrol.

* Correspondence to: Dr Neal M. Davies, Department of Pharmaceutical Sciences, College of Pharmacy, Washington State University, PO Box 646534, Pullman, WA 99164-6534, USA.
E-mail: ndavies@wsu.edu
Contract/grant sponsor: Summer Undergraduate Research Fellowship (SURF) from Washington State University College of Pharmacy and ASPET.
Contract/grant sponsor: AFPE Gateway Research Scholarship.
Contract/grant sponsor: Organic Center.

Received 21 May 2007
Revised 11 June 2007
Accepted 12 June 2007

made primarily from dried grape berries used to treat cardiovascular and other ailments (Paul *et al.*, 1999). Pterostilbene also appears to be a constituent of the stem bark of *Guibourtia tessmanii*, a tree found in central Africa that is commonly used in folk medicine (Fuendjiep *et al.*, 2002).

Due to pterostilbene's close structural similarity to resveratrol and its use in traditional medicine, pterostilbene may possess potential health benefits. Other research groups have begun to elucidate some of these benefits of pterostilbene including antioxidant, anticancer, antidiabetic and hypolipidemic activities. These groups have shown pterostilbene possesses significant antioxidant activity *in vitro* comparable to resveratrol (Rimando *et al.*, 2002; Stivala *et al.*, 2001). Additionally, pterostilbene has been reported to have cancer chemopreventive properties in *in vitro* and in *in vivo* experiments. In these experiments, pterostilbene was shown to inhibit growth, to inhibit adhesion, to inhibit metastatic growth, and to be an active apoptotic agent on certain cancer cell types (Ferrer *et al.*, 2005; Tolomeo *et al.*, 2005). Recently, pterostilbene has been identified as an inhibitor of CYP1A1, a cytochrome P450 thought to have a role in carcinogenesis, and therefore, pterostilbene may reduce the risk of mutagenesis and cancer (Mikstacka *et al.*, 2007). Pertaining to antidiabetic activity, *Pterocarpus marsupium* extract and pterostilbene alone have demonstrated ability to lower blood glucose levels (Grover *et al.*, 2005; Manickam *et al.*, 1997). Finally, pterostilbene has been shown to possess hypolipidemic properties by lowering levels of low density lipoprotein (LDL) and increasing levels of high density lipoprotein (HDL) in plasma of hamsters fed pterostilbene (Rimando *et al.*, 2005).

To our knowledge, there have been no studies evaluating the pharmacokinetics, disposition or the *in vitro* metabolism of pterostilbene. It is the objective of the present study to examine the pharmacokinetic disposition of pterostilbene as well as its *in vitro* metabolism. To facilitate this, a high performance liquid chromatographic method was developed and validated for quantification of pterostilbene in biological matrices using fluorescence detection (Remsberg *et al.*, 2007). Additionally, the objective was to further investigate pterostilbene's anticancer activity in five different cancer cell lines and antioxidant capacity via different methods as previously reported. For the first time, to our knowledge, the study aimed to examine the antiinflammatory activity of pterostilbene in two *in vitro* models using canine chondrocytes to induce and modulate arthritis and HT-29 cells (colorectal adenocarcinoma) to induce and modulate colitis. Finally, the analgesic activity of pterostilbene was investigated for the first time.

MATERIALS AND METHODS

Chemicals and reagents. *Trans*-pterostilbene and pinosylvin were purchased from Sequoia Research Products Ltd (Oxford, UK). Additional *trans*-pterostilbene was provided by Dr Agnes Rimando. HPLC grade methanol, acetonitrile and water were purchased from J. T. Baker (Phillipsburg, NJ, USA). Halothane, trypsin, ethylene diamine tetraacetic acid (EDTA), trypan blue, resazurin, sodium bicarbonate, 4-(2-hydroxyethyl)-1-piperazineethanesulfonic acid (HEPES), sodium pyruvate, penicillin-streptomycin, Dulbecco's Modified Eagle Medium (D-MEM), RMPI 1640 medium, McCoy's 5A medium, Dulbecco's Modified Eagle's Medium/Nutrient Mixture F-12 Ham (DMEM/F-12) without phenol red were purchased from Sigma (St Louis, MO, USA). Fetal bovine serum (FBS) was purchased from Equitech-Bio Inc. (Kerrville, TX, USA).

Rats were obtained from Simonsen Laboratories (Gilroy, CA, USA). Mice were purchased from Harlan Sprague-Dawley Laboratories (Indianapolis, IN, USA).

Canine chondrocytes (CnC) were purchased from Cell Applications, Inc. (San Diego, CA, USA). A-375 (malignant melanoma), HCT-116 (colorectal carcinoma), Hep-G2 (hepatocellular carcinoma), MDA-MB-231 (estrogen receptor negative breast adenocarcinoma), PC-3 (prostate adenocarcinoma) and HT-29 (colorectal adenocarcinoma) were obtained from American Type Culture Collection (ATCC, Manassas, VA, USA).

The nitric oxide (NO) quantitation kit was purchased from Active Motif (Carlsbad, CA, USA), the prostaglandin E_2 (PGE_2) ELISA kit was purchased from Amersham Biosciences Corp. (Piscataway, NJ, USA), the sulfated glycosaminoglycans (sGAG) assay kit was purchased from Kamiya Biomedical Company (Seattle, WA, USA), the soluble collagen (Sircol) assay kit was purchased from Accurate Chemical & Scientific Corp. (Westbury, NY, USA), the matrix metalloproteinase-3 (MMP-3) ELISA kit was purchased from RayBiotech Inc. (Norcross, GA, USA), the interleukin-6 (IL-6) ELISA kit, tumor necrosis factor-α (TNF-α) ELISA kit, and antioxidant assay kit were purchased from Cayman Chemical Company (Ann Arbor, MI, USA).

Chromatographic system and conditions. The HPLC system used was a Shimadzu HPLC (Kyoto, Japan) consisting of an LC-10AD pump, a SIL-10A auto injector, a RF-535 fluorescence detector and a SCL-10A system controller. Data collection and integration were achieved using a Shimadzu CR501 chromatopac integrator. The analytical column used was a Phenomenex C_{18} (250 × 4.60 mm). The mobile phase consisted of acetonitrile and HPLC water (50:50, v/v) that was filtered and degassed under reduced pressure prior to use. Separation was carried out isocratically at ambient temperature and a flow rate of 1 mL/min, with fluorescence detection excitation at 330 nm and emission at 374 nm. This HPLC method has been validated and published (Remsberg *et al.*, 2007). Validation indicated the precision of the assay was <15% (CV), and was within 14% at the limit of quantitation (0.5 μg/mL). The bias of the assay was lower than 14%, and was within 9% at the limit of quantitation.

LC/MS analysis. In order to support the presence of a pterostilbene phase II metabolite, an Agilent 1100 Series LC/MSD using API-ES (atmospheric pressure ionization – electrospray) was employed. The sample preparation and chromatographic methods were the same as detailed below. A positive-specific ion mode (SIM) was used to monitor the single plot transitions (*m/z*) of pterostilbene from 256 to 257. The presence of a glucuronide was supported by an increase in *m/z* ratio of 176. Therefore, the single plot transitions (*m/z*) for the pterostilbene glucuronide from 432 to 433 support the presence of this metabolite.

DOI: 10.1002/ptr

Animals and surgical procedures. Male Sprague-Dawley rats (250–270 g) were obtained from Simonsen Laboratories (Gilroy, CA) and allowed food (Purina Rat Chow 5001) and water *ad libitum* in our animal facility for at least 3 days before use. Rats were housed in temperature-controlled rooms with a 12 h light/dark cycle. The day before the pharmacokinetic experiment the right jugular veins of the rats were catheterized with sterile silastic cannulae (Dow Corning, Midland, MI) under halothane (Sigma Chemical Co., St Louis, MO) anesthesia. This involved exposure of the vessel prior to cannula insertion. After cannulation, the Intramedic PE-50 polyethylene tubing (Becton, Dickinson and Company, Franklin Lakes, NJ) connected to the cannula was exteriorized through the dorsal skin. The cannula was flushed with 0.9% saline. The animals were transferred to metabolic cages and fasted overnight.

Male NIH Swiss mice (20–35 g) purchased from Harlan Sprague-Dawley Laboratories (Indianapolis, IN, USA) were housed five per cage with food and water *ad libitum* in our animal facility. Mice were housed under standard conditions (22 °C room temperature, 33% humidity) and a 12 h light/dark cycle (lights on 7:00 am to 7:00 pm). Mice were kept in the holding room for at least 4 days following arrival in the facility. Animals were used only one time for each analgesic test.

Animal ethics approval was obtained from The Institutional Animal Care and Use Committee at Washington State University, in accordance with 'Principles of laboratory animal care' (NIH publication No. 85-23, revised 1985).

Rat liver microsomes preparation. Male rat liver microsomes were prepared from adult male Sprague-Dawley rats as described previously (Roupe *et al.*, 2004; Teng *et al.*, 2003). Fresh rat livers were excised from euthanized rats and put into ice-cold saline, weighed and minced. Samples were homogenized using a motorized homogenizer (four strokes) in ice-cold homogenization buffer (50 mM pH 7.4 potassium phosphate buffer, 250 mM sucrose, 1 mM EDTA) and centrifuged at 7700 × **g** for 15 min at 4 °C. The supernatant was centrifuged again at 85 600 × **g** for 1 h at 4 °C to yield microsome pellets. The microsomes were resuspended in microsome washing buffer (10 mM pH 7.4 potassium phosphate buffer, 0.1 mM EDTA and 150 mM KCl) and centrifuged again at 85 600 × **g** for 1 h at 4 °C to yield microsomes. The microsome pellet was then resuspended in 250 mM sucrose, aliquoted in vials (0.5 mL/vial), and stored at –80 °C until use. The protein concentration of the microsomal protein was determined using a protein assay (Bio-Rad, Hercules, CA, USA) using bovine serum albumin as a standard.

Phase II metabolism. The incubation procedures for measuring uridine diphosphate-glucuronosyltransferase (UGT) activities using microsomes were as follows: (1) microsomes (final concentration ~0.05 mg protein/mL) were mixed with each of the following: $MgCl_2$ (0.88 mm), saccharolactone (4.4 mm) and alamethicin (0.022 mg/mL). 42 μM (10 μg/mL) pterostilbene in a 50 mM potassium phosphate buffer (pH 7.4) was added as the substrate and finally uridine diphosphoglucuronic acid (3.5 mm) was added to activate the reaction, (2) the mixture was incubated at 37 °C for 10, 20, 30 or 60 min. The reaction was stopped by the addition of 50 μL of 94% acetonitrile/6% glacial acetic acid. Samples were centrifuged and stored at –20 °C until analysis by HPLC (Roupe *et al.*, 2004).

Dosages. No pharmacokinetic studies are reported in the literature for pterostilbene; however, pharmacokinetic studies on other stilbenes have reported i.v. dosage ranges from 10 to 20 mg/kg (Asensi *et al.*, 2002; Marier *et al.*, 2002; Roupe *et al.*, 2006a,b). For the *in vitro* studies, a 100 fold concentration range of 1–100 μg/mL was used. It is believed that these concentrations would be feasible *in vivo* due to protein binding which would limit the amount of free pterostilbene. No data on pterostilbene protein binding have been reported; however, resveratrol has been shown to bind albumin highly which is synergized by the presence of fatty acids (Jannin *et al.*, 2004). From this, it is speculated that pterostilbene might also bind albumin. For the cell culture experiments, it is assumed that pterostilbene might bind the albumin present in fetal bovine serum (FBS) of the cell media leading to concentrations similar to those possibly seen *in vivo*. For the analgesic study, a dosage of 50 mg/kg in mice was used. Literature reports of analgesic testing of polyphenols in rodents have used dosages ranging from below 1 mg/kg to more than 200 mg/kg (dos Santos *et al.*, 2006; Gadotti *et al.*, 2006; Meotti *et al.*, 2006).

Pharmacokinetic study. Male Sprague Dawley rats (n = 4, average weight 250 g) were cannulated as described in the Animals and Surgical Procedures section. The animals were placed in metabolic cages where they recovered overnight and were fasted for 12 h before dosing. The next day, the animals were dosed intravenously with pterostilbene (20 mg/kg) in polyethylene glycol (PEG) 600. This dose has been observed to exert pharmacological activity previously (Asensi *et al.*, 2002; Marier *et al.*, 2002; Roupe *et al.*, 2006b). After dosing, a series of blood samples (0.3 mL) was collected at 0, 1, 30 min, then 1, 2, 4, 6, 12, 24, 48, 72, 96 and 120 h. The cannula was flushed with 0.9% saline after each sample collection. The samples were collected into regular polypropylene microcentrifuge tubes, centrifuged at 5000 rpm for 5 min (Beckman Microfuge centrifuge, Beckman Coulter Inc., Fullerton, CA, USA), and the serum was collected. The serum was divided into two 0.1 mL fractions into separate pre-labeled regular polypropylene microcentrifuge tubes and labeled as free and total serum samples and stored at –20 °C until further sample preparation for HPLC analysis. Urine samples were also collected at 0, 2, 6, 12, 24, 48, 72, 96 and 120 h following pterostilbene administration. The volumes of urine were recorded and two 0.1 mL aliquots were collected into separate pre-labeled regular polypropylene microcentrifuge tubes and labeled as free and total urine samples and stored at –20 °C until further sample preparation for HPLC analysis. The experimental protocols were approved by the Institutional Animal Care and Use Committee of Washington State University.

Serum and urine sample preparation. Serum and urine samples (0.1 mL) were run in duplicate with or without the addition of 40 μL of 500 U/mL β-glucuronidase from *Escherichia coli* type IX-A and incubated in a shaking water bath at 37 °C for 2 h to liberate any glucuronide

DOI: 10.1002/ptr

conjugates (Yang *et al.*, 2002) The proteins present in the serum samples were precipitated using 1 mL of ice-cold HPLC-grade acetonitrile, vortexed for 1 min (Vortex Genie-2, VWR Scientific, West Chester, PA, USA) and centrifuged at 5000 rpm for 5 min (Beckman Microfuge centrifuge, Beckman Coulter Inc., Fullerton, CA, USA), the supernatant was transferred to new labeled 2 mL centrifuge tubes. The samples were evaporated to dryness under compressed nitrogen gas. The residue was reconstituted with 400 μL of mobile phase, vortexed for 1 min and centrifuged at 5000 rpm for 5 min, the supernatant was transferred to HPLC vials and 150 μL was injected into the HPLC system.

β-glucuronidase from *Escherichia coli* type IX-A cleaves specifically the glucuronidated metabolite back to the stilbenoid pterostilbene. Therefore, the samples without enzymatic hydrolysis (free samples) were utilized to determine the concentration of pterostilbene, whereas the samples with enzymatic hydrolysis (total samples) were utilized to determine the concentration of the pterostilbene originally present plus the concentration of the glucuronidated metabolite cleaved back to pterostilbene by the action of the enzyme. Finally, by subtracting the free sample concentration from the total sample, the concentration of the glucuronidated metabolite can be calculated.

Pharmacokinetic analysis. Pharmacokinetic analysis was performed using data from individual rats for which the mean and standard error of the mean (SEM) were calculated for each group. The elimination rate constant KE was estimated by linear regression of the serum concentrations in the log-linear terminal phase. In order to estimate the serum concentrations (C_0) immediately after i.v. dosing, a two-compartmental model was fitted to the serum concentration versus time data using WinNonlin® software (Ver. 5.1). The estimated C_0 was then used with the actual measured serum concentrations to determine the area under the serum concentration-time curve (AUC). The $AUC_{0-\infty}$ was calculated using the combined log-linear trapezoidal rule for data from time of dosing to the last measured concentration, plus the quotient of the last measured concentration divided by KE/2.303. Non-compartmental pharmacokinetic methods were used to calculate the different pharmacokinetic parameters in the terminal phase, namely clearance (CL_{total}, dose divided by $AUC_{0-\infty}$) and volume of distribution (Vd_{β}, CL_{total} divided by KE). Based on the cumulative urinary excretion, the fraction excreted in urine (F_e = total cumulative amount of pterostilbene excreted in urine, $\sum Xu$, divided by the dose), renal clearance (CL_{renal}, F_e multiplied by CL_{total}), hepatic clearance ($CL_{hepatic}$, CL_{renal} subtracted from CL_{total}, assuming that hepatic clearance is equivalent to non-renal clearance), extraction ratio (ER, $CL_{hepatic}$ divided by mean hepatic blood flow, Q). The mean hepatic blood flow (Q) is approximately 3.22 L/h/kg (Davies and Morris, 1993) and using the hematocrit in rat (Davies *et al.*, 1993) of 0.48, this yields a mean hepatic plasma flow of 1.74 L/h/kg.

Antioxidant capacity determination. The antioxidant capacity of pterostilbene was measured through an assay that relies on the inhibition of the oxidation of ABTS (2,2′-azino-di-[3-ethylbenzthiazoline sulphonate]) to $ABTS^{+}$ by metmyoglobin. The amount of $ABTS^{+}$ can be monitored spectrophotometrically, and the degree of suppression of absorbance caused by the antioxidants is proportional to their concentration, which is expressed as millimolar Trolox equivalents. For this assay, pterostilbene was dissolved in DMSO on the day of the experiment to yield concentrations of 1, 10, 50 and 100 μg/mL. No further dilution in medium was employed. To run the test, 10 μL of sample was combined with 10 μL of metmyoglobin and 150 μL of chromogen. Then, 40 μL of hydrogen peroxide working solution was added within 1 min to all the samples. The plate was covered and incubated on a shaker for 5 min at room temperature, and the absorbance was measured at 750 nm. For more information please refer to the instruction in the kit (Anti-Oxidant Assay Kit from Cayman Chemical – cat. No. 709091).

Cell culture. A-375 (malignant melanoma) and MDA-MB-231 (estrogen receptor negative breast adenocarcinoma) cell lines were maintained in Dulbecco's Modified Eagle Medium (D-MEM) and supplemented with 10% heat-inactivated fetal bovine serum (FBS), penicillin-streptomycin solution (10 mL/L), HEPES (2.4 g/L) and sodium pyruvate (110.4 mg/L). HCT-116 (colorectal carcinoma) and HT-29 (colorectal adenocarcinoma) cell lines were maintained in McCoy's 5A medium and supplemented with 10% heat-inactivated FBS, penicillin-streptomycin solution (10 mL/L) and HEPES (6.0 g/L). Hep-G2 (human hepatoma) cell line was maintained in Dulbecco's Modified Eagle Medium: Nutrient Mixture F-12 (Ham) (DMEM/F-12) and supplemented with 10% heat-inactivated fetal bovine serum (FBS), penicillin-streptomycin solution (10 mL/L) and insulin (4 mg/mL). The PC-3 (prostate adenocarcinoma) cell line was maintained in RPMI medium and supplemented with 10% heat-inactivated FBS and penicillin-streptomycin solution (10 mL/L). CnC (canine chondrocytes) cell line was maintained in DMEM/F-12 without phenol red supplemented with 20% heat-inactivated fetal bovine serum (FBS) and penicillin-streptomycin solution (10 mL/L). All cell lines were incubated at 37 °C in a 5% CO_2 atmosphere.

Cell subculture. Thirty minutes prior to subculturing the corresponding medium for each cell line, phosphate buffered saline (PBS) and trypsin-ethyl diamine tetetric acid (EDTA) solution comprised 0.5% trypsin, 0.2% EDTA/0.9% NaCl diluted in PBS to prepare a 10% working solution were placed in a 37 °C water bath. Next, the cell flask was removed from the 5% CO_2 incubator and cells were observed under the light microscope to determine the percentage of confluence, and overall appearance and growth. The desired percentage of confluence was 50–75%. After confluence was determined, medium was aspirated and cells were washed with 5 mL PBS. PBS was aspirated and 2 mL of the trypsin-EDTA working solution was added and the flask was placed in the 5% CO_2 incubator (37 °C) for 2 min. The flask was then removed from the incubator and observed under the microscope to determine full cell detachment. Detached cells were transferred to a 15 mL conical tube containing 8 mL PBS. The conical tube was then centrifuged at 700 rpm for 5 min. Following centrifugation, the conical tube was removed and the PBS was aspirated, leaving the cell pellet undisturbed. Cells were resuspended in 6 mL fresh

DOI: 10.1002/ptr

media and 10 μL was removed and diluted four times in trypan blue. The cell-trypan blue solution was added to a hematocytometer and the number of live cells was counted using a cell counter. The number of dead cells was also recorded. If it was determined that the number of dead cells surpassed 10% of the total population of healthy cells, the cell line was excluded from future experiments and a new generation of the cell line was thawed.

The total number of cells present in the flask was determined using the following equation:

$$\text{Cells/mL} = (\#\ \text{cells}/4)\ (\text{dilution})\ (1 \times 10^4) \quad (1)$$

Depending on the observed cell number and the desired cell seeding number, the cells and fresh media were added in determined volumes to a fresh T75 (125 mL capacity) cell culture flask. The flask was then placed into 5% CO_2 incubator (37 °C). Cell subculture was performed 1–2 times per week depending on the growth rate of the cell line and observed confluence.

Cell number. The optimal cell seeding numbers for each cell line was determined by preliminary cell seeding number experiments. Cells were seeded in numbers 1×10^4, 2×10^4, 3×10^4 and so on until the final cell seeding number 1×10^5 per well in a 96-well plate. Cell plates were incubated at 37 °C in a 5% CO_2 atmosphere for 72 h. Following incubation, medium was aspirated and alamar blue (resazurin) fluorescent dye solution was diluted in fresh medium to make a 10% resazurin solution. The 10% solution was added directly to cells. The cell plates were incubated at 37 °C in a 5% CO_2 atmosphere for 3 h. The cell plates were subsequently removed from the incubator and placed at room temperature in a darkened drawer to protect from light for 30 min. Next, the cell plates were placed into the Cytofluor® 4000 fluorescence multi-well plate reader (Applied Biosystems, USA). Fluorescence was read at an excitation of 485 nm and an emission of 530 nm. Standard curves of cell seeding number against fluorescence were generated. Canine chondrocytes, MDA-MD-231, Hep-G2 and PC-3 cell lines were seeded at 5000 cells/well. A-375 cell line was seeded at 1000 cells/well, while HCT-116 cell line was seeded at 3000 cells/well. The HT-29 cell line was seeded at 20 000 cells/well.

Alamar blue assay. Alamar blue (resazurin) fluorescent dye is a facile and accurate assay to determine the cytotoxicity of many cell lines including the five cancer cell lines used in the present study (O'Brien *et al.*, 2000). The resazurin non-fluorescent compound is metabolized into the fluorescent compound resorufin by intact and viable cells. This emission of fluorescence can be quantified using a cell plate reader and the number of viable cells following treatment can be determined. Cells were counted and seeded on 96-well plates. The seeded cells were incubated at 37 °C in a 5% CO_2 atmosphere for 24 h. Pterostilbene was dissolved in dimethyl sulfoxide (DMSO) on the day of the experiment and was diluted in medium to yield concentrations of 1, 10, 50 and 100 μg/mL. Following aspiration of the medium, cells were treated with the pterostilbene solution. Additional cells were treated with either DMSO diluted in medium or medium only. Treated and control cells were incubated at 37 °C in a 5% CO_2 atmosphere for 72 h. After cell plates were removed from the incubator, the medium was aspirated and replaced with 10% alamar blue (resazurin) fluorescent dye diluted in fresh medium. Cell plates were incubated at 37 °C in a 5% CO_2 atmosphere for an additional 3 h. Following incubation, the cell plates were placed in a darkened environment for 30 min at room temperature. Next, the cell plates were placed into the Cytofluor® 4000 fluorescence multi-well plate reader (Applied Biosystems, USA), and fluorescence was read at an excitation of 485 nm and an emission of 530 nm. The viable cell number (as a percent of control) in each cell line exposed to varying concentrations of pterostilbene was determined. The IC_{50} values for each cell line were determined by using pharmacodynamic modeling using WinNonlin® software (Ver. 5.1).

***In vitro* colitis model.** HT-29 (colorectal adenocarcinoma) cells were counted and seeded on 96-well plates. The seeded cells were incubated at 37 °C in a 5% CO_2 atmosphere until they reached monolayer confluency of 60–80% (72 h). Cells were then serum starved for 24 h. Pterostilbene was dissolved in DMSO on the day of the experiment and was diluted in medium to yield concentrations of 1, 10, 50 and 100 μg/mL. To begin the experiment, the cells were divided into one of four groups: cells treated with vehicle (DMSO in media) in the presence of TNF-α, cells treated with vehicle (DMSO in media) without TNF-α, cells treated with pterostilbene in the presence of TNF-α (1–100 μg/mL), and cells treated with pterostilbene without TNF-α (1–100 μg/mL). Following aspiration of the medium, cells were treated with either pterostilbene (1–100 μg/mL) or vehicle. Cells were then also treated with either 50 μL TNF-α (20 ng/mL) or 50 μL of blank media. Media from each well was collected 24 h later. Prostaglandin E_2 (PGE_2) levels were measured within 72 h using commercially available ELISA kits.

***In vitro* chondrocyte inflammation model.** Canine chondrocytes (CnC) were counted and seeded on 96-well plates. The seeded cells were incubated at 37 °C in a 5% CO_2 atmosphere for 24 h. Pterostilbene was dissolved in DMSO on the day of the experiment and was diluted in medium to yield concentrations of 1, 10, 50 and 100 μg/mL. Following aspiration of the medium, the cells were treated with 100 μL of interleukin-1β (IL-1β) (10 ng/mL) to induce inflammation, the plates were incubated at 37 °C in a 5% CO_2 atmosphere for 2 h. Following incubation, the cells were treated with pterostilbene (1–100 μg/mL). Additional cells were treated with either DMSO diluted in medium or medium only. Treated and control cells were incubated at 37 °C in a 5% CO_2 atmosphere for 72 h. After the cell plates were removed from the incubator, the medium was collected and stored at –80 °C until further analysis.

Medium collected was analysed by the levels of five key mediators released during inflammatory events including nitric oxide (NO), prostaglandin E_2 (PGE_2), sulfated glycosaminoglycans (sGAG), matrix metalloproteinase-3 (MMP-3) and tumor necrosis factor-α (TNF-α). Quantitation kits were used to determine all levels of mediators. Nitric oxide (NO) was measured as nitrate and nitrite levels utilizing Griess reagent, sulfated glycosoaminoglycans (sGAG) utilizing the Alcian blue dye method; and prostaglandin E_2

DOI: 10.1002/ptr

(PGE_2), tumor necrosis factor-α (TNF-α), and matrix metalloproteinase-3 (MMP-3) were measured utilizing separate commercial ELISA kits.

Analgesia analysis. Male NIH Swiss mice (20–35 g) were divided into a control group to receive vehicle ($n = 5$) and a treatment group to receive a 50 mg/kg dose of pterostilbene ($n = 5$). Due to its poor water solubility, pterostilbene was prepared in an emulsion of 5% Tween 80 in normal saline at a final concentration of 50 mg/kg. The strength of the pterostilbene emulsion was 5 mg/mL, which resulted in approximately 0.2–0.3 mL injected into each mouse. The control group received a vehicle of 5% Tween 80 in normal saline. After dosing each animal intraperitoneal (i.p.), 15 min was allowed to pass before the tail-flick and hot-plate tests were completed. The animals were tested one at a time and were not habituated to the particular device before testing. Animals were only used once for each test.

For the tail flick test, an automated tail flick apparatus (Model TF6, EMDIE Instrument, Maidens, VA, USA) was used which elicited a response by applying radiant heat to the dorsal surface of the tail. For the experiment, each mouse was gently held and an automatic timer measured latency until the mouse flicked its tail away from the source of the light. The heat stimulus was set to provide a pre-drug tail-flick response time of 3–4 s. The cutoff time for the heat stimulus was set at 10 s to avoid tissue damage (Emmanouil and Quock, 1989).

The hot plate test was undertaken on a hot plate analgesiometer (I.I.T.C., Woodland Hills, CA, USA) with a Plexiglas enclosure (30 cm long × 30 cm wide × 45 cm high). The temperature at the hot plate surface was held at a consistent temperature of 52 °C. The latency between when the mice were dropped on the heated surface and the time when paw licking or escape behavior first occurred was measured. The animal was then immediately removed from the surface. A maximum cutoff time of 60 s was employed (Hodges *et al.*, 1994) .

Statistical analysis. Compiled data were presented as mean and standard error of the mean (mean ± SEM). Where possible, the data were analysed for statistical significance using NCSS Statistical and Power Analysis software (NCSS, Kaysville, UT). Student's *t*-test was employed for unpaired samples with a value of $p < 0.05$ being considered statistically significant. Comparisons among means were tested using General Linear Models (GLM) ANOVA followed by the Newman-Keuls multiple-comparison test with a value of $p < 0.05$ being considered statistically significant.

RESULTS AND DISCUSSION

Metabolism in rat liver microsomes under a UGT generating system

The HPLC method was applied to the determination of pterostilbene and its metabolic products in the phase II metabolic kinetic study of pterostilbene (10 μg/mL) in rat liver microsomes. Following the incubation of pterostilbene with rat liver microsomes and UGT enzyme at 37 °C, there was a decrease in concentration of pterostilbene suggesting glucuronidation of pterostilbene. This decrease became most apparent after 30 min of incubation. The HPLC method was able to detect a peak of a metabolite at approximately 6 min. Incubation of a 60 min sample with β-glucuronidase showed a decrease in the peak of the metabolite providing further evidence of phase II metabolism. Mass spectrometry supported the presence of a glucuronidated metabolite with molecular ion at *m/z* 433.

Pharmacokinetic study

Standard curves demonstrated linearity over the concentration range studied for the serum and urine samples, and chromatograms were free of interference from endogenous components. Total samples (incubated with β-glucuronidase from *Escherichia coli* Type IX-A) demonstrated the presence of a glucuronidated metabolite based on the increase in pterostilbene (aglycone parent compound) concentrations after the enzymatic hydrolysis in both serum and urine. Further mass spectrometry supported the presence of the glucuronidated metabolite with molecular ion *m/z* 433. Glucuronidation of pterostilbene agrees with previous rat and human kinetic studies on resveratrol that concluded resveratrol exists predominately in its conjugated form in both plasma and urine (Wenzel and Somoza, 2005).

The serum concentration vs time profile for pterostilbene demonstrated a rapid decline in concentrations in the first hour, representing a distribution phase, which was followed by a steady elimination phase up to 6 h, after which the serum concentrations were below detectable levels (0.05 μg/mL) (Fig. 2A). The glucuronidated pterostilbene metabolite exhibited an increase in concentration at 1–2 h, indicating the possibility of enterohepatic recycling of the metabolite. Enterohepatic recycling has previously been reported for resveratrol (Marier *et al.*, 2002).

Table 1 summarizes the pharmacokinetic parameters exhibited by pterostilbene at a dose of 20 mg/kg. Non-compartmental analysis in WinNonlin® software (Ver. 5.1) was used to model both serum and urine data. The total serum clearance of pterostilbene was determined to be 0.960 ± 0.025 L/h/kg. The fraction excreted in urine (Fe) was determined to be 0.219 ± 0.088%, indicating that pterostilbene is mainly excreted via non-renal routes. This represents that renal clearance

Table 1. Pharmacokinetic parameters of pterostilbene in the rat

Pharmacokinetic parameter	Mean ± SEM
AUC_{inf} (ug.h/mL)	17.5 ± 6.6
Vd_{β} (L/kg)	2.41 ± 1.13
$CL_{hepatic}$ (L/h/kg)	0.958 ± 0.025
CL_{renal} (L/h/kg)	0.002 ± 0.001
CL_{total} (L/h/kg)	0.960 ± 0.025
F_e (%)	0.219 ± 0.088
KE (h^{-1}) serum	0.697 ± 0.367
KE (h^{-1}) urine	0.058 ± 0.027
$t_{1/2}$ (h) serum	1.73 ± 0.78
$t_{1/2}$ (h) urine	17.3 ± 5.6
MRT (h)	0.837 ± 0.323
Extraction ratio (ER)	0.551 ± 0.014

DOI: 10.1002/ptr

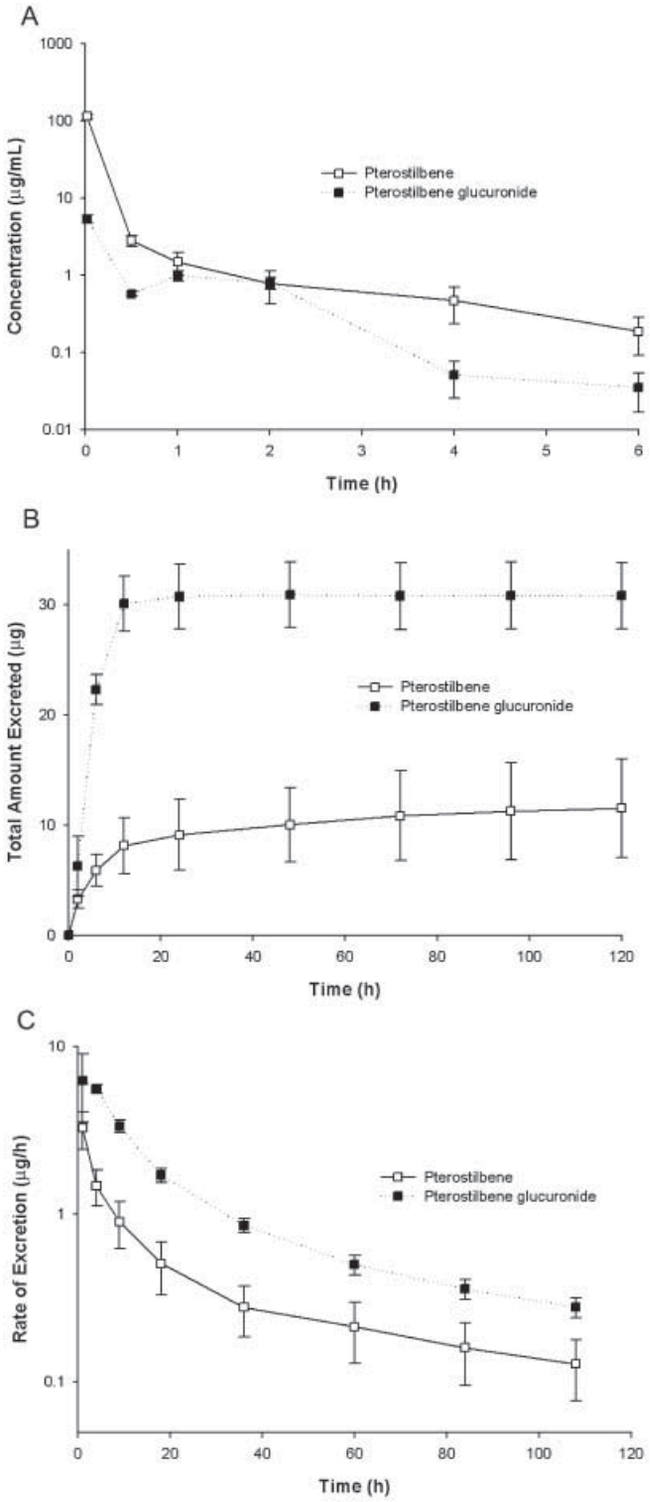

Figure 2. (A) Pterostilbene disposition in serum following intravenous administration; (B) cumulative pterostilbene and glucuronidated metabolite (μg) excreted in urine over 120 h; (C) rate of excretion (μg/h) of pterostilbene and glucuronidated metabolite in urine over 120 h (n = 4 mean ± SEM).

(CL_{renal}) was 0.002 ± 0.001 L/h/kg, and hepatic clearance ($CL_{hepatic} = CL_{total} - CL_{renal}$) was determined to be 0.958 L/h/kg ($CL_{hepatic} = 0.960 - 0.002$) assuming that non-renal clearance equals hepatic clearance. The volume of distribution of pterostilbene was determined to be 2.41 ± 1.13 L/kg suggesting that pterostilbene resides predominately in the central blood compartment. The mean area under the curve (AUC) representing the total amount of drug exposure in the serum over time was 17.5 ± 6.6 μg.h/mL. The serum concentrations of pterostilbene declined rapidly with a mean elimination half-life of 1.73 ± 0.78 h. This is in agreement with the half-life previously reported for resveratrol of less than 1 h (Asensi *et al.*, 2002).

Analysis of urine samples showed the presence of the parent compound pterostilbene and the glucuronidated metabolite previously identified in serum (Fig. 2B, 2C). The total cumulative urinary excretion plot (Fig. 2B) indicates that pterostilbene is excreted predominantly in the glucuronidated form. The glucuronidated metabolite appears to be mostly excreted by 12 h post-dose, while the amount of pterostilbene (parent compound) excreted in urine steadily increased even at 120 h post-dose. The half-life of pterostilbene in urine was determined to be 17.3 ± 5.6 h. The discrepancy of the serum half-life (1.73 ± 0.78 h) and the urinary half-life (17.3 ± 5.6 h) suggests that the serum half-life is likely underestimating the overall half-life of pterostilbene due to assay sensitivity limitations and overestimation of terminal elimination rate constant. This phenomenon has previously been reported in the pharmacokinetic study of other stilbenes (Roupe *et al.*, 2006b). The rate of urinary excretion plot (Fig. 2C) indicates that pterostilbene and its glucuronidated metabolite have similar rates of excretion as indicated by their parallel slopes (-KE/2.303).

The total dose of pterostilbene administered was 20 mg/kg. The average weight of the rats in this experiment was ~250 g. This translates to approximately each rat administered 5 mg of pterostilbene. The plot of total amount excreted shows that the amount of pterostilbene and the glucuronidated metabolite excreted (~11.5 and 30.8 μg, respectively) are very small compared with the overall dose administered (~5 mg). This suggests that pterostilbene is eliminated predominately via non-renal routes. The fraction excreted unchanged (F_e) was 0.219 ± 0.088%, and therefore CL_{renal} was 0.002 ± 0.001 (L/h/kg). Urinary excretion accounts for approximately 0.219% of total unchanged pterostilbene excreted further suggesting that non-renal excretion predominates (99.78% of total pterostilbene excreted). Excretion via non-renal routes for pterostilbene agrees with literature reports of non-renal excretion of resveratrol (Marier *et al.*, 2002).

Antioxidant capacity of pterostilbene

Figure 3 reports the antioxidant capacity of pterostilbene in units of Trolox equivalents. The baseline or DMSO only samples have a very low antioxidant capacity (0.009 mM ± 0.001). Pterostilbene demonstrates a concentration-dependent antioxidant activity with an antioxidant capacity at 1 μg/mL (0.004 mM) of 0.124 mM Trolox equivalents and a capacity at 100 μg/mL (0.4 mM) of 0.360 mM Trolox equivalents. This indicates that pterostilbene prevents oxidation at comparable levels to Trolox, if not better (as seen at lower concentrations). The ability of pterostilbene to inhibit oxidation of ABTS agrees with the work of other groups that have shown pterostilbene's ability to scavenge 2,2-diphenyl-1-picrylhydrazyl (DPPH) radicals (Stivala *et al.*, 2001) and 2,2′-azo-bis(2-amidinopropane) (ABAP) derived peroxyl radicals (Rimando *et al.*, 2002).

DOI: 10.1002/ptr

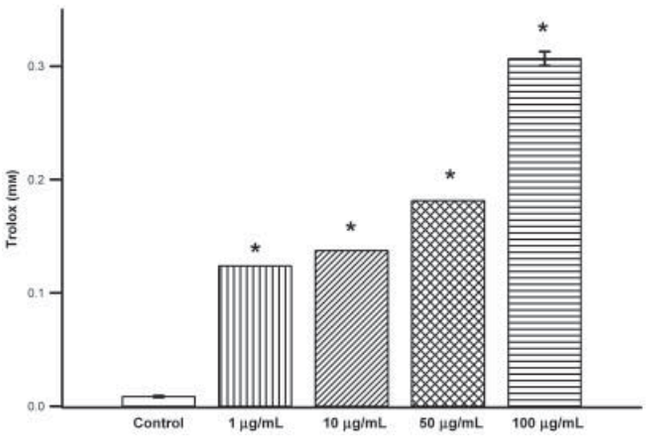

Figure 3. Antioxidant capacity (mean ± SEM) of pterostilbene at 1, 10, 50 and 100 µg/mL dissolved in DMSO. * Significantly different from baseline (DMSO) samples ($p < 0.05$).

The ability of pterostilbene to work as an antioxidant is of utmost importance as the wide range of health benefits of polyphenols are speculated to result from their antioxidant capacity. For instance, the ability of resveratrol to limit the start and progression of atherosclerosis is associated with resveratrol's ability to inhibit the oxidation of polyunsaturated fatty acids (PUFA) (Fremont, 2000). High levels of resveratrol and other polyphenols in red wine is thought to be responsible for the French paradox in which red wine drinkers have a reduced incidence of coronary heart disease (Das *et al.*, 1999). It is likely that the health benefits associated with pterostilbene are due to its antioxidant capacity.

Anticancer activity of pterostilbene

The anticancer activity of pterostilbene was tested in A-375 (malignant melanoma), HCT-116 (colorectal carcinoma), Hep-G2 (hepatocellular carcinoma), MDA-MB-231 (estrogen receptor negative breast adenocarcinoma) and PC-3 (prostate adenocarcinoma) cell lines by measuring cell viability after treatment with pterostilbene (1, 10, 50 and 100 µg/mL). Analysis of cell viability as a percent of the control following exposure showed concentration-dependent activity in all cell lines tested (Fig. 4). The IC_{50} of each cell line was determined by using pharmacodynamic modeling using WinNonlin® software (Ver. 5.1). Pterostilbene had the greatest activity against the Hep-G2 cell line with an IC_{50} of 4.09 ± 3.05 µg/mL (16.0 µM). Pterostilbene was also active in MDA-MB-231 (IC_{50} = 10.4 ± 3.8 µg/mL (40.6 µM)) and HCT-116 (IC_{50} = 11.6 ± 0.8 µg/mL (45.3 µM)). Moderate activity was observed in A-375 (IC_{50} = 108 ± 6 µg/mL (421 µM)) and it was not active in PC-3 (IC_{50} = 1006 ± 239 µg/mL (3.9 mM)). The pharmacokinetic parameters reported above indicate that pterostilbene will likely obtain the highest concentration in the liver and the colon as it is likely excreted via non-renal routes. The cancers of the regions studied included Hep-G2 (liver) and HCT-116 (colon) cancers, against which pterostilbene showed high activity.

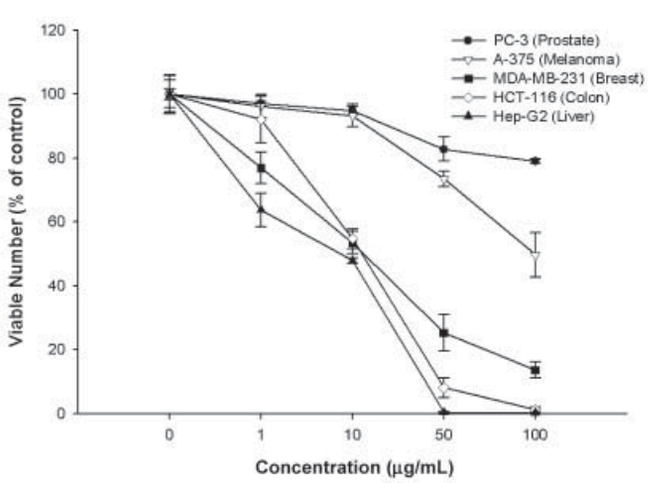

Figure 4. Viable cell numbers after administration of pterostilbene (0–100 µg/mL) in five cancer cell lines (mean ± SD).

It was previously shown that pterostilbene and other stilbenoid compounds were not cytotoxic against normal human umbilical vein endothelial cells (HUVEC) (Roupe unpublished). Therefore, this demonstrated anticancer effect agrees with the work of other groups that have shown the ability of pterostilbene to inhibit proliferation and to be an apoptosis inducer in certain cancer cell types (Ferrer *et al.*, 2005; Tolomeo *et al.*, 2005).

In vitro colitis model

To experimentally mimic the inflammatory disease, colitis, inflammation was induced in adenocarcinoma (HT-29) cells by introducing TNF-α into the cell medium. Simultaneously, pterostilbene (1–100 µg/mL) was introduced into the cell medium. Collected media were assessed for PGE_2 levels. Samples induced by TNF-α showed a marked increase in the PGE_2 levels compared with samples not induced by TNF-α (Fig. 5). Pterostilbene reduced the levels of PGE_2 in a concentration-dependent manner in samples induced with inflammation and those in which no TNF-α was added. Reduction in the inflammatory mediator PGE_2, may be indicative of possible amelioration of colitis *in vivo*, as PGE_2 plays a significant role in inflammatory bowel disease (Otani *et al.*, 2006).

It has been further suggested that suppression of prostaglandin synthesis likely leads to reduction in colonic cancer (Gustafson-Svard *et al.*, 1997). The reduction of PGE_2 demonstrated by pterostilbene in this model may demonstrate protective effects of pterostilbene against colon cancer, which agrees with a recent study where pterostilbene was shown in rats to suppress the formation of aberrant crypt foci, early cellular biomarkers of colon cancer development (Suh *et al.*, 2007).

Chondrocyte inflammation model

Figure 6 reports the levels of MMP-3, nitric oxide, sGAG, PGE_2 and TNF-α in cell media of canine chondrocytes. It was observed that treatment with pterostilbene (1–100 µg/mL) is able to attenuate some of the inflammatory mediators induced by IL-1β. Controls for each mediator showed a low level of mediator production which markedly increased after treatment with IL-1β. Pterostilbene treatment resulted in concentration-dependent inhibition of MMP-3 production

DOI: 10.1002/ptr

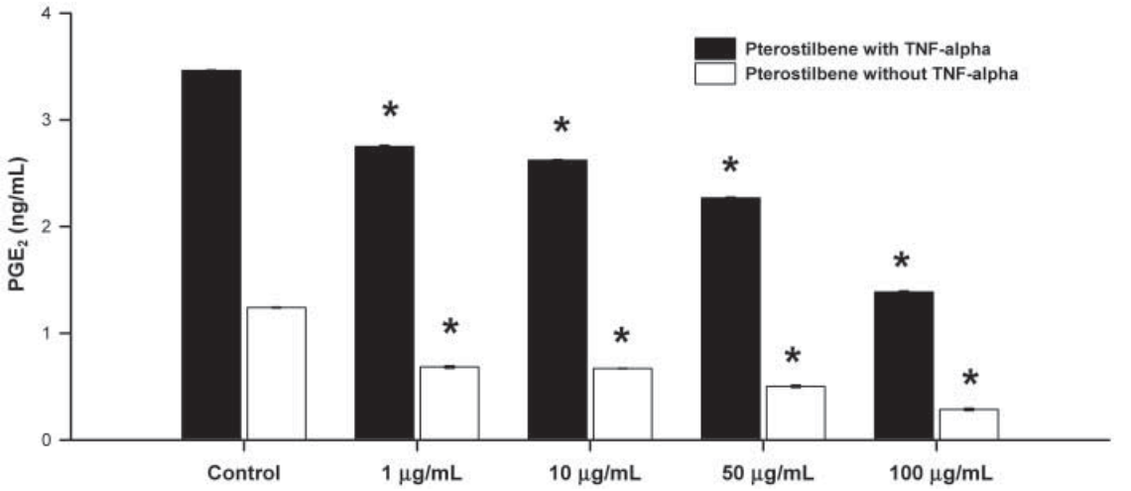

Figure 5. Prostaglandin E_2 (PGE_2) production (mean ± SEM) in the cell culture medium from HT-29 cells 24 h after the addition of pterostilbene at 1–100 μg/mL. Values are expressed as μg/mL. * Significantly different from control samples ($p < 0.05$).

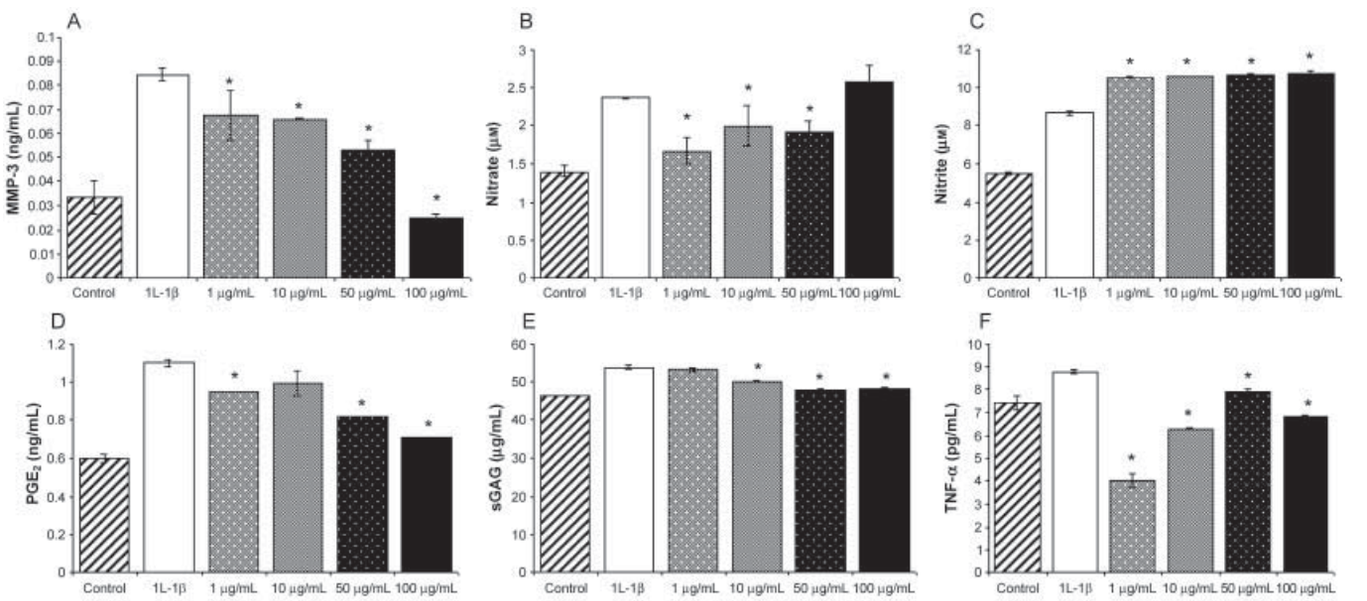

Figure 6. Analysis of inflammatory mediators in the cell culture medium from canine chondrocytes 72 h after the addition of pterostilbene at 1–100 μg/mL with IL-1β (100 μL of 100 ng/mL). (A) Matrix metalloproteinase-3 (MMP-3) production (mean ± SEM). Values are expressed as ng/mL. (B) Nitrate production (mean ± SEM). Values are expressed as μM. (C) Nitrite production (mean ± SEM). Values are expressed as μM. (D) Prostaglandin E_2 (PGE_2) production (mean ± SEM). Values are expressed as ng/mL. (E) Sulfated glycosaminoglycans (sGAG) release (mean ± SEM). Values are expressed as μg/mL. (F) Tumor necrosis factor-α (TNF-α) production (mean ± SEM). Values are expressed as pg/mL. * Significantly different from IL-1β treated samples ($p < 0.05$).

(Fig. 6A). Conversely, pterostilbene treatment yielded an initial decrease in the levels of nitrate followed by a concentration-dependent increase (Fig. 6B). Levels of nitrite were maintained at levels higher than the IL-1β controls, regardless of the concentration of pterostilbene (Fig. 6C). PGE_2 levels followed a Gaussian distribution with all concentrations having decreased levels of PGE_2 compared with the IL-1β control (Fig. 6D). Levels of sGAG showed a mild concentration-dependent decrease (Fig. 6E). TNF-α levels demonstrated a skewed Gaussian distribution with all concentrations having lower levels compared with the IL-1β control (Fig. 6F).

Arthritis results from the presence of degenerative, inflammatory and oxidative stress mechanisms that cause an imbalance between the reparative and destructive cycles in cartilage. To study these pathogenetic mechanisms, certain mediators were examined, including PGE_2 and TNF-α for inflammation, and MMP-3, sGAG, and NO for chondro-degeneration. Antioxidant capacity as mentioned above is indicative of ability to counteract oxidative stress.

Pterostilbene decreased the levels of MMP-3, sGAG, PGE_2 and TNF-α compared with the IL-1β control levels of these mediators. As sGAG and MMP-3 are linked to cartilage degradation, pterostilbene may be able to down-regulate these mediators, and therefore, limit the process of joint degradation. Furthermore, pterostilbene may reduce inflammation and oxidative stress as indicated by a reduction in PGE_2 and TNF-α levels and high antioxidant capacity. More studies are needed to determine if this ability is seen *in vivo*. Studies of resveratrol indicate it may be important for the prevention and treatment of arthritis as it is involved in the down-regulation of many inflammatory gene products (Khanna *et al.*, 2007), and it has been shown in a

DOI: 10.1002/ptr

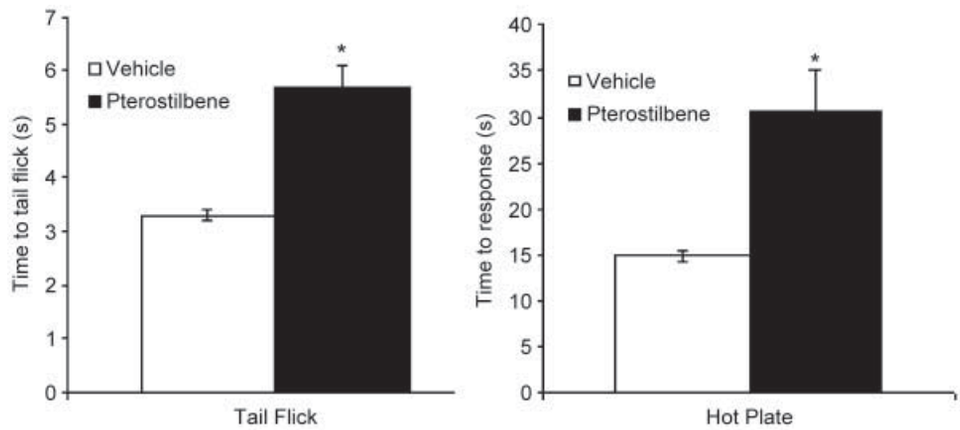

Figure 7. Analgesic activity of pterostilbene (mean ± SEM) at a 50 mg/kg dose assessed via the tail-flick and hot-plate tests. * Significantly different from control mice ($p < 0.05$).

rabbit osteoarthritis model to reduce significantly cartilage tissue destruction (Khanna *et al.*, 2007).

Analgesic activity

Figure 7 presents the analgesic activity of pterostilbene as assessed through the tail-flick and hot plate tests. Pretreatment of mice with pterostilbene (50 mg/kg, i.p.) increased the latency period to response in both tests (tail-flick by 2.4 s and hot-plate by 15.8 s). Gupta *et al.* used the hot plate test to show resveratrol possesses significant antinociception by influencing the opioidergic mechanism (Gupta *et al.*, 2004). Given the similarities in structure, pterostilbene may produce its effect through the opioid receptor. Conversely, the analgesic effect may be through pterostilbene's ability to inhibit cyclooxygenase (COX). Rimando *et al.* reported that pterostilbene moderately inhibited COX-1 and weakly inhibited COX-2 (Rimando *et al.*, 2002). Hougee *et al.*, however, reported a much higher activity of COX-2 inhibition of *Pterocarpus marsupium* extract, which was related to pterostilbene content (Hougee *et al.*, 2005). Based on these observations, it seems that pterostilbene provides its analgesic effect based on its potential to modulate COX-1 and COX-2.

CONCLUSIONS

In summary, the pharmacokinetics in rats and the *in vitro* metabolism of pterostilbene were evaluated for the first time. Additionally, it was determined that pterostilbene possesses anticancer activity, antioxidant activity, antiinflammatory activity in canine chondrocytes and HT-29 cells, as well as analgesic activity in mice. Further exploration of the pharmacodynamics of pterostilbene is under way to demonstrate utility in the targeted treatment of gastrointestinal and liver disorders such as ulcerative colitis, Crohn's disease, cirrhosis, colorectal cancer, hyperlipidemia and hepatitis, given the inherent pharmacokinetic affinity for this stilbene to the reticuloendothelial system.

Acknowledgements

The authors would like to acknowledge the Summer Undergraduate Research Fellowship (SURF) from Washington State University College of Pharmacy and ASPET awarded to CMR, an AFPE Gateway Research Scholarship awarded to CMR, and an unrestricted grant from the Organic Center awarded to NMD. We would also like to acknowledge the initial technical assistance from Drs Kathryn Roupe and Todd Taruscio.

REFERENCES

Adrian M, Jeandet P, Douillet-Breuil AC, Tesson L, Bessis R. 2000. Stilbene content of mature *Vitis vinifera* berries in response to Uv-C elicitation. *J Agric Food Chem* **48**: 6103–6105.

Asensi M, Medina I, Ortega A *et al.* 2002. Inhibition of cancer growth by resveratrol is related to its low bioavailability. *Free Radic Biol Med* **33**: 387–398.

Das DK, Sato M, Ray PS *et al.* 1999. Cardioprotection of red wine: role of polyphenolic antioxidants. *Drugs Exp Clin Res* **25**: 115–120.

Davies B, Morris T. 1993. Physiological parameters in laboratory animals and humans. *Pharm Res* **10**: 1093–1095.

dos Santos MD, Almeida MC, Lopes NP, de Souza GE. 2006. Evaluation of the anti-inflammatory, analgesic and antipyretic activities of the natural polyphenol chlorogenic acid. *Biol Pharm Bull* **29**: 2236–2240.

Douillet-Breuil AC, Jeandet P, Adrian M, Bessis R. 1999. Changes in the phytoalexin content of various *Vitis* spp. in response to ultraviolet C elicitation. *J Agric Food Chem* **47**: 4456–4461.

Emmanouil DE, Quock RM. 1989. Modification of nitrous oxide analgesia by benzodiazepine receptors. *Anesth Prog* **36**: 5–8.

Ferrer P, Asensi M, Segarra R *et al.* 2005. Association between pterostilbene and quercetin inhibits metastatic activity of B16 melanoma. *Neoplasia* **7**: 37–47.

Fremont L. 2000. Biological effects of resveratrol. *Life Sci* **66**: 663–673.

Fuendjiep V, Wandji J, Tillequin F *et al.* 2002. Chalconoid and stilbenoid glycosides from *Guibourtia tessmanii*. *Phytochemistry* **60**: 803–806.

Gadotti VM, Tibola D, Flavia Paszcuk A, Rodrigues AL, Calixto JB, Santos AR. 2006. Contribution of spinal glutamatergic receptors to the antinociception caused by agmatine in mice. *Brain Res* **1093**: 116–122.

Grover JK, Vats V, Yadav SS. 2005. *Pterocarpus Marsupium* extract (Vijayasar) prevented the alteration in metabolic

patterns induced in the normal rat by feeding an adequate diet containing fructose as sole carbohydrate. *Diabetes Obes Metab* **7**: 414–420.

Gupta YK, Sharma M, Briyal S. 2004. Antinociceptive effect of *trans*-resveratrol in rats: involvement of an opioidergic mechanism. *Methods Find Exp Clin Pharmacol* **26**: 667–672.

Gustafson-Svard C, Lilja I, Hallbook O, Sjodahl R. 1997. Cyclooxygenase and colon cancer: clues to the aspirin effect? *Ann Med* **29**: 247–252.

Hodges BL, Gagnon MJ, Gillespie TR *et al.* 1994. Antagonism of nitrous oxide antinociception in the rat hot plate test by site-specific mu and epsilon opioid receptor blockade. *J Pharmacol Exp Ther* **269**: 596–600.

Hougee S, Faber J, Sanders A *et al.* 2005. Selective Cox-2 inhibition by a pterocarpus marsupium extract characterized by pterostilbene, and its activity in healthy human volunteers. *Planta Med* **71**: 387–392.

Jannin B, Menzel M, Berlot JP, Delmas D, Lancon A, Latruffe N. 2004. Transport of resveratrol, a cancer chemopreventive agent, to cellular targets: plasmatic protein binding and cell uptake. *Biochem Pharmacol* **68**: 1113–1118.

Khanna D, Sethi G, Ahn KS *et al.* 2007. Natural products as a gold mine for arthritis treatment. *Curr Opin Pharmacol* **7**: 344–351.

Kodan A, Kuroda H, Sakai F. 2002. A stilbene synthase from Japanese red pine (*Pinus Densiflora*): implications for phytoalexin accumulation and down-regulation of flavonoid biosynthesis. *Proc Natl Acad Sci USA* **99**: 3335–3339.

Manickam M, Ramanathan M, Jahromi MA, Chansouria JP, Ray AB. 1997. Antihyperglycemic activity of phenolics from *Pterocarpus Marsupium*. *J Nat Prod* **60**: 609–610.

Marier JF, Vachon P, Gritsas A, Zhang J, Moreau JP, Ducharme MP. 2002. Metabolism and disposition of resveratrol in rats: extent of absorption, glucuronidation, and enterohepatic recirculation evidenced by a linked-rat model. *J Pharmacol Exp Ther* **302**: 369–373.

Meotti FC, Missau FC, Ferreira J *et al.* 2006. Anti-allodynic property of flavonoid myricitrin in models of persistent inflammatory and neuropathic pain in mice. *Biochem Pharmacol* **72**: 1707–1713.

Mikstacka R, Przybylska D, Rimando AM, Baer-Dubowska W. 2007. Inhibition of human recombinant cytochromes P450 Cyp1a1 and Cyp1b1 by *trans*-resveratrol methyl ethers. *Mol Nutr Food Res* **51**: 517–524.

O'Brien J, Wilson I, Orton T, Pognan F. 2000. Investigation of the Alamar blue (resazurin) fluorescent dye for the assessment of mammalian cell cytotoxicity. *Eur J Biochem* **267**: 5421–5426.

Otani T, Yamaguchi K, Scherl E *et al.* 2006. Levels of Nad(+)-dependent 15-hydroxyprostaglandin dehydrogenase are reduced in inflammatory bowel disease: evidence for involvement of Tnf-alpha. *Am J Physiol Gastrointest Liver Physiol* **290**: G361–G368.

Paul B, Masih I, Deopujari J, Charpentier C. 1999. Occurrence of resveratrol and pterostilbene in age-old Darakchasava, an Ayurvedic medicine from India. *J Ethnopharmacol* **68**: 71–76.

Pezet R, Pont V. 1988. Mise en evidence de pterostilbene dans les grappes de *Vitis vinifera* (Var. Gamay Et Pinot). *Plant Physiol Biochem* **26**: 603–607.

Remsberg CM, Yanez JA, Roupe KA, Davies NM. 2007. High-performance liquid chromatographic analysis of pterostilbene in biological fluids using fluorescence detection. *J Pharm Biomed Anal* **43**: 250–254.

Rimando AM, Cuendet M, Desmarchelier C, Mehta RG, Pezzuto JM, Duke SO. 2002. Cancer chemopreventive and antioxidant activities of pterostilbene, a naturally occurring analogue of resveratrol. *J Agric Food Chem* **50**: 3453–3457.

Rimando AM, Kalt W, Magee JB, Dewey J, Ballington JR. 2004. Resveratrol, pterostilbene, and piceatannol in vaccinium berries. *J Agric Food Chem* **52**: 4713–4719.

Rimando AM, Nagmani R, Feller DR, Yokoyama W. 2005. Pterostilbene, a new agonist for the peroxisome proliferator-activated receptor alpha-isoform, lowers plasma lipoproteins and cholesterol in hypercholesterolemic hamsters. *J Agric Food Chem* **53**: 3403–3407.

Roupe K, Remsberg C, Yanez J, Davies N. 2006a. Pharmacometrics of stilbenes: seguing towards the clinic. *Curr Clin Pharmacol* **1**: 81–101.

Roupe K, Teng XW, Fu X, Meadows GG, Davies NM. 2004. Determination of piceatannol in rat serum and liver microsomes: pharmacokinetics and Phase I and Ii biotransformation. *Biomed Chromatogr* **18**: 486–491.

Roupe KA, Yanez JA, Teng XW, Davies NM. 2006b. Pharmacokinetics of selected stilbenes: rhapontigenin, piceatannol and pinosylvin in rats. *J Pharm Pharmacol* **58**: 1443–1450.

Stivala LA, Savio M, Carafoli F *et al.* 2001. Specific structural determinants are responsible for the antioxidant activity and the cell cycle effects of resveratrol. *J Biol Chem* **276**: 22586–22594.

Suh N, Paul S, Hao X *et al.* 2007. Pterostilbene, an active constituent of blueberries, suppresses aberrant crypt foci formation in the azoxymethane-induced colon carcinogenesis model in rats. *Clin Cancer Res* **13**: 350–355.

Teng XW, Cutler DJ, Davies NM. 2003. Kinetics of metabolism and degradation of mometasone furoate in rat biological fluids and tissues. *J Pharm Pharmacol* **55**: 617–630.

Tolomeo M, Grimaudo S, Di Cristina A *et al.* 2005. Pterostilbene and 3′-hydroxypterostilbene are effective apoptosis-inducing agents in Mdr and Bcr-Abl-expressing leukemia cells. *Int J Biochem Cell Biol* **37**: 1709–1726.

Wenzel E, Somoza V. 2005. Metabolism and bioavailability of *trans*-resveratrol. *Mol Nutr Food Res* **49**: 472–481.

Yang C, Tsai S, Chao P, Yen H, Chien T, Hsiu S. 2002. Determination of hesperetin and its conjugate metabolites in serum and urine. *J Food Drug Anal* **10**: 143–148.